Acta Cryst. (1998). D**54**, 409–412

Crystallization and preliminary high-resolution X-ray diffraction analysis of native and β-mercaptoethanol-inhibited urease from *Bacillus pasteurii*

STEFANO BENINI,[a]† STEFANO CIURLI,[a]‡ WOJCIECH R. RYPNIEWSKI,[b] KEITH S. WILSON[c] AND STEFANO MANGANI[d]‡ at [a]*Institute of Agricultural Chemistry, University of Bologna, Viale Berti Pichat 10 I-40127 Bologna, Italy,* [b]*European Molecular Biology Laboratory, c/o DESY, Notkestrasse 85, D-22603 Hamburg, Germany,* [c]*Department of Chemistry, University of York, Heslington, York YO1 5DD, England, and* [d]*Department of Chemistry, University of Siena, Pian dei Mantellini, 44 I-53100 Siena, Italy*

(*Received 17 July 1997; accepted 3 October 1997*)

Abstract

Hexagonal crystals of urease from *Bacillus pasteurii* have been obtained by vapour diffusion at 293 K in 20 m*M* Tris–HCl, neutral pH, containing 50 m*M* Na_2SO_3. Isomorphous crystals of urease inhibited with β-mercaptoethanol were also obtained by including 4 m*M* of the inhibitor in the enzyme solution. Crystals of the native and inhibited enzyme diffract, respectively, to 2.00 Å (96.7% completeness) and to 1.65 Å (98.7% completeness) using synchrotron X-ray cryogenic (100 K) conditions. The space group is $P6_322$ for both forms, and the unit-cell parameters are $a = b = 131.36$, $c = 189.76$ Å for native urease and $a = b = 131.34$, $c = 190.01$ Å for inhibited urease. Under the same conditions, single crystals of *B. pasteurii* urease inhibited with acetohydroxamic acid, cisteamine and phenylphosphorodiamidate were also obtained.

1. Introduction

Urease (urea aminohydrolase E.C. 3.5.1.5), the enzyme that catalyzes the hydrolysis of urea at a rate 10^{14} times faster than the rate of the uncatalyzed reaction (Hausinger, 1993), may be thought to represent the paradigm in the development of biological inorganic chemistry. The first enzyme to be crystallized, from the plant source *Canavalia ensiformis* (jack bean) (Sumner, 1926), was the first protein shown to contain nickel in the active site (Dixon *et al.*, 1975). This discovery stimulated efforts to unravel the chemistry of such a rare microelement in other biological settings, leading to the discovery of the presence of nickel in CO-dehydrogenase (Drake *et al.*, 1980), methyl coenzyme *M* reductase-bound factor Ni-F430 (Diekert *et al.*, 1980; Whitman & Wolfe, 1980), and Ni,Fe-hydrogenase (Lancaster, 1982). In the absence of structural models of the urease active site, the synthetic analogue approach was utilized to obtain small coordination compounds of known structure featuring spectroscopic and functional properties as similar as possible to the enzymatic system (Stemmler *et al.*, 1995; Wages *et al.*, 1993).

Recently, the report of the X-ray structure of urease from a bacterial source, *Klebsiella aerogenes* (Jabri *et al.*, 1995), together with the structure of the apoenzyme and three active-site mutants (Jabri & Karplus, 1996; Park *et al.*, 1996), has finally provided a detailed picture of the active site. In *K. aerogenes* urease, a heteropolymeric protein with an $\alpha_3\beta_3\gamma_3$ quaternary structure, the two Ni^{II} ions, known to be present in the active site, (Todd & Hausinger, 1987) are in the α subunit: one Ni cation appears to be bound to $His^{\alpha 246}$ through the N^{δ} atom and to $His^{\alpha 272}$ through N^{ε}, while the other Ni cation is bound to $His^{\alpha 134}$ and $His^{\alpha 136}$ through N^{ε}, to $Asp^{\alpha 360}$ through $O^{\delta 1}$, and to one water molecule. The two Ni ions are held close to each other (at 3.5 Å) by a bridging carboxylate group of the carbamylated $Lys^{\alpha 217}$ residue (Jabri *et al.*, 1995). The structure of native *K. aerogenes* urease suggests the presence of one tricoordinated pseudotetrahedral Ni cation (with low occupancy of the fourth site by a water molecule) and one pentacoordinated distorted trigonal bipyramidal Ni cation. This conclusion is in disagreement with all previous spectroscopic data on *K. aerogenes* and jack-bean ureases (Alagna *et al.*, 1984; Blakeley *et al.*, 1983; Clark & Wilcox, 1989; Clark *et al.*, 1990; Finnegan *et al.*, 1991; Hasnain & Piggot, 1983; Wang *et al.*, 1994), which pointed to the presence of hexa- or pentacoordinated slightly distorted octahedral Ni cations.

Urease from *Bacillus pasteurii*, a highly ureolytic and alkaliphilic soil bacterium (Gibson, 1935), was the first urease isolated from bacterial sources (Larson & Kallio, 1954). This enzyme is heteropolymeric (Benini, Gessa *et al.*, 1996) [$M_r(\alpha) = 61.4$, $M_r(\beta) = 14.0$, $M_r(\gamma) = 11.1$ kDa (Moersdorf *et al.*, 1994)] and features an active site containing two Ni cations (Benini, Gessa *et al.*, 1996). The primary structures of *B. pasteurii* (Moersdorf *et al.*, 1994) and *K. aerogenes* (Mulrooney & Hausinger, 1990) ureases are highly homologous [63% (α), 46% (β) and 61% (γ), respectively], and the amino-acid residues ligating the Ni cations in *K. aerogenes* urease are conserved in the enzyme from *B. pasteurii* (Moersdorf *et al.*, 1994). In contrast to the reported structure of native *K. aerogenes* urease, Ni-edge X-ray absorption spectroscopy (XAS) studies, carried out on *B. pasteurii* urease, suggest an average coordination environment of the Ni ions represented by five or six N/O ligands arranged in a pseudo-octahedral geometry, (Benini, Ciurli *et al.*, 1996), with two of the ligands being histidine imidazole side chains.

The inconsistencies between the spectroscopic and structural analyses of urease might be resolved by determining the number and position of light, non-protein ligands in the vicinity of the metal ions, which could be represented by water molecules or by hydroxide ions bound to the Ni cations either in an end-on or a bridging mode. Given the relatively low resolution (2.2 Å) and completeness (92%) of the structure of urease from *K. aerogenes* (Jabri *et al.*, 1995), it is possible that such ligands could not be clearly detected in the proximity of the electron-rich dinuclear Ni center. This point is of fundamental importance in understanding the catalytic mechanism of urea hydrolysis, for which the role of water molecules (or

† Present address: European Molecular Biology Laboratory, c/o DESY, Notkestrasse 85, D-22603 Hamburg, Germany.
‡ Corresponding authors. E-mail addresses: mangani@unisi.it, sciurli@agrsci.unibo.it.

hydroxide ions) present in the active site may be crucial (Zerner, 1991). Data with higher resolution and completeness should also be useful in resolving the discrepancies between the coordination geometry of Ni^{II} found in urease and the stereoelectronic behavior of this metal cation in synthetic coordination compounds, for which no cases of coordination geometry analogous to that proposed for *K. aerogenes* urease are known. Another reason to establish with high accuracy the structure of ureases isolated from different sources is to allow a comparison, essential in establishing the existence of common features. These will provide a better understanding of the chemistry of the catalysis and also allow rational design of inhibitors capable of functioning with a broad range of microbial ureases, in order to decrease the negative effects of urea hydrolysis in both medical and agricultural applications (Mobley & Hausinger, 1989).

In this paper we report the crystallization, synchrotron X-ray data collection at cryogenic temperature and the solution of the structure of *B. pasteurii* urease, both in the native state and in the presence of the inhibitor β-mercaptoethanol, as the first step toward the determination of the structure of the active site at high resolution.

2. Materials and methods

2.1. *Protein purification and crystallization*

B. pasteurii urease was isolated and purified to a specific activity of *ca* 2500 units mg^{-1} as previously reported (Benini, Gessa *et al.*, 1996). Crystallization trials on the native enzyme were performed at 293 K by the hanging-drop method, using 3 µl of a 11 mg ml^{-1} urease solution in 20 m*M* Tris–HCl, pH = 7.5, containing 50 m*M* Na_2SO_3, and diluting this volume with 3 µl of precipitant solution. The drop was equilibrated by vapor diffusion against 0.6 ml of precipitant solution using a Hampton Research 24-well Linbro plate.

Numerous, very small crystals of *B. pasteurii* native urease were observed after 7 d at 277 K using 30%(*v*/*v*) 2-methyl-2,4-pentanediol (MPD) in 0.1 *M* sodium acetate, pH = 4.6, containing 0.02 *M* $CaCl_2$ as precipitant; no further crystal growth occurred. Using 28%(*v*/*v*) polyethylene glycol (PEG) 400 (Sigma) in 0.1 *M* Hepes, pH = 7.5, containing 0.2 *M* $CaCl_2$, small crystals formed after 7 d at 277 K, but again no further growth was observed. The same result was obtained using 30% PEG 1500 (Sigma) as precipitant. Using 55% saturated ammonium sulfate in 20 m*M* Tris–HCl, pH = 7.0, at 277 K, very thin hexagonal plates formed.

In the effort to increase growth in the third dimension of crystals obtained in the latter conditions, a whole range of co-precipitants were tried. Successful and reproducible crystallizations were obtained at 293 K using 53% saturated ammonium sulfate solution containing 1.2 *M* LiCl, in 20 m*M* sodium citrate, pH = 6.3. Colorless crystals grew to about 0.2 × 0.2 × 0.6 mm on average after 4 d, together with the formation of some amorphous material. The crystals were 'rice shaped' (Fig. 1), exhibiting faces and hexagonal bipyramidal geometry only rarely. Using the same crystallization conditions, but including 4 m*M* β-mercaptoethanol in the urease solution, well shaped single crystals having on average dimensions of about 0.3 × 0.3 × 0.7 mm and the same habit as the ones formed in the absence of this inhibitor, were obtained. No amorphous material appeared in these conditions, probably indicating a higher stability of the enzyme.

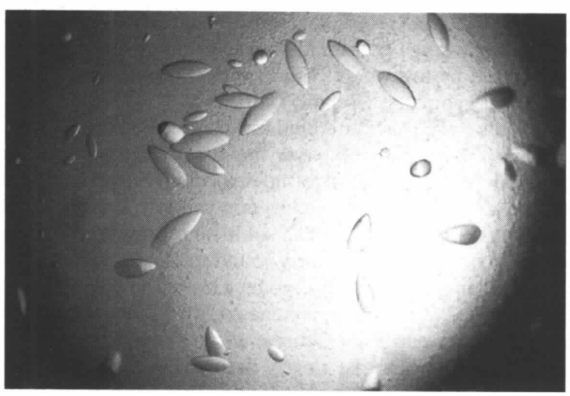

Fig. 1. Crystals of β-mercaptoethanol-inhibited urease (*ca* 0.2 × 0.2 × 0.5 mm) from *B. pasteurii*.

2.2. *Crystallographic diffraction data collection and evaluation*

A single crystal of native urease, with dimensions of 0.2 × 0.2 × 0.5 mm was transferred from the mother liquor to the cryobuffer (20% ethylene glycol in the precipitant solution). After *ca* 1 min, the crystal was scooped into a rayon cryoloop, and rapidly exposed to a cold nitrogen stream (Oxford Cryosystems Cryostream) on the BW7B wiggler line (λ = 0.8855 Å) of the DORIS storage ring at the EMBL outstation at the Deutsches Elektronen Synchrotron (DESY) in Hamburg (Germany). Diffraction data were collected at 100 K using a 30 cm MAR Research imaging-plate scanner (Hamburg, Germany). An analogous procedure was used for a single crystal (0.4 × 0.4 × 0.7 mm) of the β-mercaptoethanol-inhibited urease. For both native and inhibited urease, one crystal was sufficient to complete data collection. Each data set was recorded in two sweeps, at different exposure times, in order to accurately record both the stron-

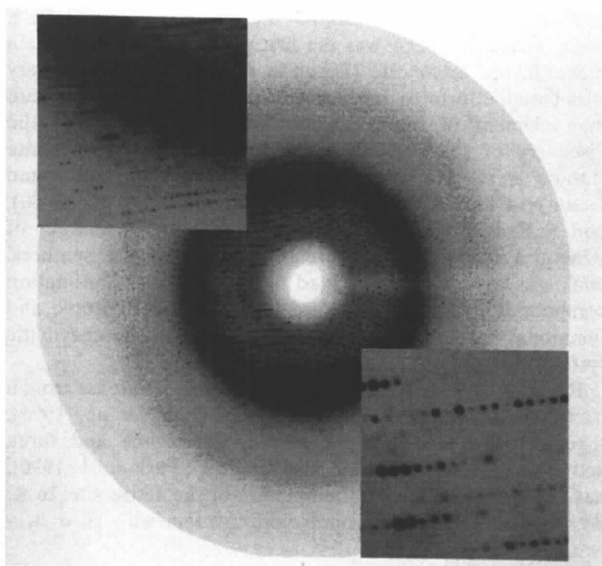

Fig. 2. Diffraction pattern from an oscillation image of β-mercaptoethanol-inhibited urease from *B. pasteurii*. Insets show details of the image at higher magnification.

Table 1. *Summary of data collection and evaluation for B. pasteurii urease*

	Native		Inhibited	
	'High'	'Low'	'High'	'Low'
Number of images	71	35	80	31
Oscillation angle (°)	0.3	1	0.4	1
Exposure time (s)	*ca* 240	*ca* 160	*ca* 240	*ca* 120
Maximum resolution (Å)	2.0		1.65	
Wavelength (Å)	0.8855			
R_{merge}† (%)	9.7		7.6	
Raw measurements used	836977		1172081	
Unique reflections	63765		114679	
Completeness (%)	96.7 (20–2.0 Å)		98.7 (14–1.65 Å)	
Completeness in high-resolution shell (5)	95.4 (2.02–2.0 Å)		97.8 (1.68–1.65 Å)	
Greater than 2σ (%)	78.2		80.2	
Greater than 2σ at high resolution (%)	55.2 (2.03–2.0 Å)		46.4 (1.68–1.65 Å)	
I/σ at high resolution	2.4 (2.03–2.00 Å)		2.2 (1.68–1.65 Å)	
Space group	$P6_322$			
Postrefined cell parameters (Å)				
$a = b$	131.36		131.34	
c	189.76		190.01	

† $R_{merge} = \sum_i |I_i - \langle I \rangle| / \sum \langle I \rangle$, where I_i is an individual intensity measurement, and $\langle I \rangle$ is the average intensity for this reflection with summation over all the data.

gest, low-resolution, and the weakest, high-resolution, diffraction intensities. The reflections measured in the diffraction pattern of native and β-mercaptoethanol-inhibited urease were processed with *DENZO* and merged with *SCALEPACK* (Otwinowski, 1993).

3. Results and discussion

3.1. *Data collection and evaluation*

Both native and inhibited urease crystals gave high-resolution diffraction patterns, but at room temperature they rapidly decayed in the intense X-ray synchrotron beam. Data collection was thus carried out using cryogenic conditions (Hope, 1990; Rogers, 1994; Watenpaugh, 1991), which lead to improvement in quality and resolution of the data, as evidenced in Fig. 2 for inhibited urease.

Data at 2.00 Å (96.7% completeness) and at 1.65 Å (98.7% completeness) resolution were obtained for native and inhibited enzymes, respectively. Table 1 reports a summary of data collection and statistics for both native and inhibited urease. Assuming one $\alpha\beta\gamma$ fragment (86.5 kDa) per asymmetric unit, the volume-to-mass ratio, V_m, is 2.7 $Å^3\,Da^{-1}$, giving a solvent content of 54%. These values are in the normal range found for proteins (Matthews, 1968), and compare well with the corresponding values determined for *K. aerogenes* urease (2.2 $Å^3\,Da^{-1}$ and 45%, respectively), indicating that four urease $\alpha_3\beta_3\gamma_3$ molecules lie on the special positions of point symmetry 3 present in the cell. The unit-cell parameters (Table 1) were not significantly different between the crystals of the native and the inhibited urease.

3.2. *Molecular replacement*

The program *AMoRe* (Navaza, 1994) from the *CCP*4 program suite (Collaborative Computational Project, Number 4, 1994) was used for the molecular-replacement solution of the β-mercaptoethanol-inhibited urease. Because of the high sequence homology with the *K. aerogenes* enzyme (Jabri *et al.*, 1995) (PDB code: 1KAU), the structure of the latter was used as a search model. The rotation function was applied to the search model placed in a *P*1 cell of dimensions 90 × 90 × 90 Å, using terms between 8.0 and 3.5 Å and a Patterson search radius of 35 Å. A peak in the rotation function was obtained which gave a correlation coefficient of 12.2%; the next highest peak had a correlation coefficient of 5.4%. The translation search, applied to the best solution obtained from the translation function, provided the correct solution of the structure with a correlation coefficient of 47.4%; the second highest peak gave a correlation coefficient of only 5.5%. After rigid-body refinement, the correlation coefficient for the best solution was improved to 52.1%, with an *R* factor ($R = \sum ||F_o| - |F_c|| / \sum |F_o|$) of 42%. The initial model was built with *O* (Jones *et al.*, 1991) and the refinement of the structure is in progress. The model obtained for inhibited urease has been used as a starting model for the native urease structure refinement.

The very high quality achieved in data collection, remarkable given the very high molecular weight of the protein (260 kDa), should provide a clear basis for understanding structure–function relationships in urease. In particular, the precise location of the water molecules in the active site of the native enzyme, will help us to understand the catalytic mechanism of this important hydrolytic enzyme, while the binding mode of β-mercaptoethanol will clarify the mechanism of inhibition, thus allowing the development of new inhibitors by structure-based molecular design. The availability of crystals of urease inhibited with acetohydroxamic acid, cisteamine, and phenylphosphorodiamidate constitutes the basis for further investigation of the mode of binding of known inhibitors to the active site of this nickel-containing metalloenzyme.

The authors thank the European Union for support of the work at EMBL Hamburg through the HCMP Access to Large Installations Project, Contract Number CHGE-CT93-0040. SC is grateful to Consiglio Nazionale delle Ricerche, Comitato 11 'Technologie e Innovarou', for partially funding the research described in this work.

References

Alagna, L., Hasnain, S. S., Piggot, B. & Williams, D. J. (1984). *Biochem. J.* **220**, 591–595.

Benini, S., Ciurli, S., Nolting, H. F. & Mangani, S. (1996). *Eur. J. Biochem.* **239**, 61–66.

Benini, S., Gessa, C. & Ciurli, S. (1996). *Soil Biol. Biochem.* **28**, 819–821.

Blakeley, R. L., Dixon, N. E. & Zerner, B. (1983). *Biochim. Biophys. Acta*, **744**, 219–229.

Clark, P. A. & Wilcox, D. E. (1989). *Inorg. Chem.* **28**, 1326–1333.

Clark, P. A., Wilcox, D. E. & Scott, R. A. (1990). *Inorg. Chem.* **29**, 579–581.

Collaborative Computational Project, Number 4 (1994). *Acta Cryst.* D**50**, 760–763.

Diekert, G., Klee, B. & Thauer, R. K. (1980). *Arch. Microbiol.* **124**, 103–106.

Dixon, N. E., Gazzola, C., Blakeley, R. & Zerner, B. (1975). *J. Am. Chem. Soc.* **97**, 4131–4132.

Drake, H. L., Hu, S.-I. & Wood, H. G. (1980). *J. Biol. Chem.* **255**, 7174–7180.

Finnegan, M. G., Kowal, A. T., Werth, M. T., Clark, P. A., Wilcox, D. E. & Johnson, M. K. (1991). *J. Am. Chem. Soc.* **113**, 4030–4032.

Gibson, T. (1935). *Zentralbl. Bakteriol. Parasitenkd. Abt. II*, **92**, 364–380.

Hasnain, S. S. & Piggot, B. (1983). *Biochem. Biophys. Res. Commun.* **112**, 279–283.

Hausinger, R. P. (1993). *Biochemistry of Nickel*. New York: Plenum Press.

Hope, H. (1990). *Annu. Rev. Biophys. Biophys. Chem.* **19**, 107–126.

Jabri, E., Carr, M. B., Hausinger, R. P. & Karplus, P. A. (1995). *Science*, **268**, 998–1004.

Jabri, E. & Karplus, P. A. (1996). *Biochemistry*, **35**, 10616–10626.

Jones, T. A., Zou, Y. Y., Cowan, S. W. & Kjeldgaard, M. (1991). *Acta Cryst.* A**47**, 110–119.

Lancaster, J. R. Jr (1982). *Science*, **216**, 1324–1325.

Larson, A. D. & Kallio, R. E. (1954). *J. Bacteriol.* **68**, 67–73.

Matthews, B. W. (1968). *J. Mol. Biol.* **33**, 491–497.

Mobley, H. L. T. & Hausinger, R. P. (1989). *Microbiol. Rev.* **53**, 85–108.

Moersdorf, G., Weinmann, P. & Kaltwasser, H. (1994). EMBL Data Library, X78411.

Mulrooney, S. B. & Hausinger, R. P. (1990). *J. Bacteriol.* **172**, 5837–5843.

Navaza, J. (1994). *Acta Cryst.* A**50**, 157–163.

Otwinowski, Z. (1993). In *Proceedings of the CCP4 Study Weekend*, edited by L. Sawyer, N. Isaacs & S. Bailey, pp. 56–62. Warrington: Daresbury Laboratory.

Park, I.-S., Michel, L. O., Pearson, M. A., Jabri, E., Karplus, P. A., Wang, S., Dong, J., Scott, R. A., Koehler, B. P., Johnson, M. K. & Hausinger, R. P. (1996). *J. Biol. Chem.* **271**, 18632–18637.

Rogers, D. W. (1994). *Structure*, **2**, 1135–1139.

Stemmler, A. J., Kampf, J. W., Kirk, M. L. & Pecoraro, V. L. (1995). *J. Am. Chem. Soc.* **117**, 6368–6369.

Sumner, J. B. (1926). *J. Biol. Chem.* **69**, 435–441.

Todd, M. J. & Hausinger, R. P. (1987). *J. Biol. Chem.* **262**, 5963–5967.

Wages, H. E., Taft, K. L. & Lippard, S. J. (1993). *Inorg. Chem.* **32**, 4985–4987.

Wang, S., Lee, M. H., Hausinger, R. P., Clark, P. A., Wilcox, D. E. & Scott, R. A. (1994). *Inorg. Chem.* **33**, 1589–1593.

Watenpaugh, K. D. (1991). *Curr. Opin. Struct. Biol.* **1**, 1012–1015.

Whitman, W. B. & Wolfe, R. S. (1980). *Biochem. Biophys. Res. Commun.* **92**, 1196–1201.

Zerner, B. (1991). *Bioorg. Chem.* **19**, 116–131.